JOURNAL OF MAGNETIC RESONANCE, Series B 102, 222–227 (1993)

COMMUNICATIONS

Motion Artifact Compensation in ^{1}H Spectroscopic Imaging by Signal Tracking

STEFAN POSSE, CHARLES ANDRE CUENOD,* AND DENIS LE BIHAN

*Diagnostic Radiology Department and * Laboratory of Diagnostic Radiology Research, The National Institutes of Health, Building 10, Room 1C660, Bethesda, Maryland 20892*

Received March 12, 1993; revised June 1, 1993

Proton magnetic resonance spectroscopic imaging (MRSI) is increasingly being used to map metabolite concentrations in human brain *in vivo* (*1–6*). In order to avoid regions with strong magnetic field inhomogeneities and signals from free mobile fatty acids in regions surrounding the brain, volume prelocalization methods based on double spin echoes (PRESS) (*7, 8*) and stimulated echoes (STEAM) (*9–11*) are used. Motion artifacts due to changes in position from phase-encode step to phase-encode step (*view-to-view motion*) are usually negligible when head restraints are used. However, the multitude of strong gradient pulses used for volume prelocalization introduces additional motion sensitivity to displacements during the spectroscopic volume prelocalization (*intraview motion*).

Signal errors due to macroscopic intraview motion appear as phase errors and amplitude losses in individual *k*-space acquisitions, similar to view-to-view artifacts, which upon Fourier transformation lead to localization errors and signal losses. For example, it can be shown that uniform movements along one spatial direction (linear translational motion) lead to phase changes only in individual acquisitions without affecting the signal amplitude (Fig. 1e). Rotations and more complex forms of macroscopic motion lead both to signal losses and to phase shifts (Fig. 1f). In brain spectroscopy, cardiac-related brain pulsations with velocities exceeding 1 mm/s (*12–14*) as well as small head movements may introduce significant intraview artifacts when pulse sequences with several strong volume prelocalization gradient pulses are used.

Motion artifacts are even more important in the presence of additional gradient pulses, such as for diffusion measurements (*15*). For example, the signal from spins moving 1.5 mm/s in the presence of a gradient pair of 10 ms pulse width and 10 mT/m strength separated by 46 ms already experiences a phase shift of 180°. With signal averaging, such phase errors, which are usually incoherent, may lead to significant signal losses due to phase cancellation. Motion artifacts from residual water and lipid signals from superficial regions which may be much more intense than metabolite signals may lead to substantial spectral contaminations.

While motion artifacts and their compensation in conventional imaging have been extensively covered in the literature (*16–23*), few reports have addressed motion artifacts in MRSI (*24*). In this paper we present a new method for compensating phase-encoding artifacts due to macroscopic intraview object motion by detecting motion-related signal errors in the echo signal prior to phase encoding. This allows one to separate phase and amplitude errors due to intraview motion from valuable phase and amplitude information due to phase encoding. Measurements *in vivo* using a strongly motion-sensitized localization scheme demonstrate the performance of the method.

With our method, data acquisition is started immediately after the last gradient-dephasing pulse and phase-encoding gradients are applied immediately before the center of the echo (Figs. 1c and 1d). Each acquisition is stored separately to avoid phase cancellation with signal averaging. During the brief period of phase encoding, additional motion-related signal errors are negligible. Since local magnetic field gradients are usually negligible compared to applied imaging gradients, there is no significant signal rephasing during signal acquisition.

Phase errors detected in the data points acquired prior to phase encoding can be corrected by zero-order phase correction in the time domain. Amplitude errors detected in these data points can be corrected by normalizing the signal amplitudes along the *k*-space domain(s), for example, by increasing the gain in those data traces which suffer from signal losses. The data points acquired before and during phase encoding are subsequently removed by left shifting the data set to the center of the echo. A conventional spectroscopic image reconstruction is performed to obtain absorption-mode spectra. While methods based on signal tracking are most efficient for uniformly moving objects, artifacts due to nonuniform movements are more difficult

1064-1866/93 $5.00

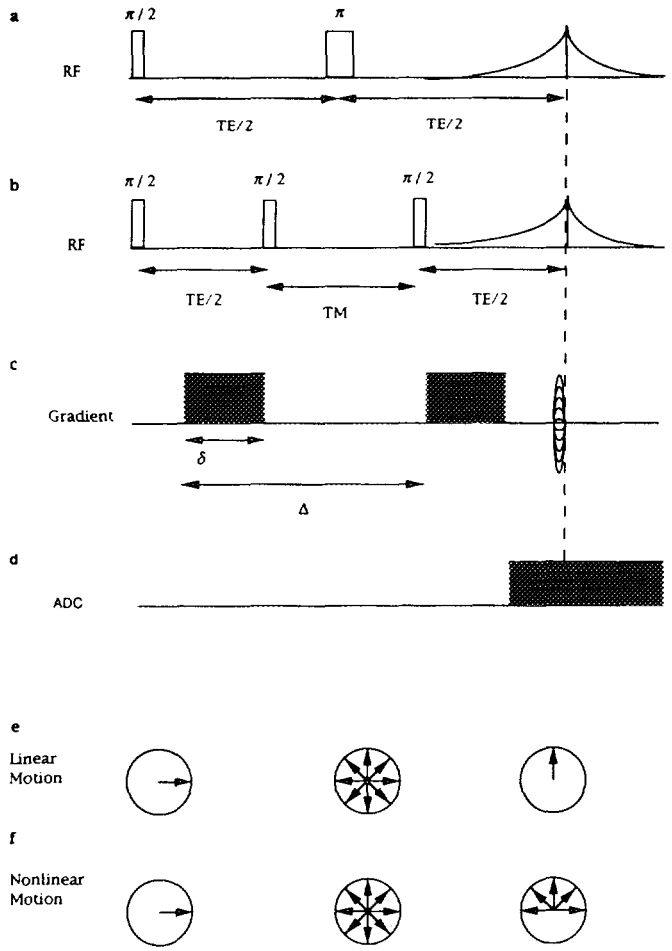

FIG. 1. Motion artifacts in spectroscopic-imaging pulse sequences and their compensation: Sequence (a) is a primary spin echo. Sequence (b) is a stimulated echo. Motion-sensitizing gradients (c) of duration δ are applied symmetrically during the TE/2 intervals. Δ is the time separation between the two gradient pulses. Phase-encoding gradients are applied immediately before the center of the echo. Data acquisition (d) starts before phase encoding to distinguish motion-related signal errors from signal modulation due to phase encoding. The symbols in (e) and (f) depict the spin magnetization in the transverse plane after excitation, after the first motion-sensitizing gradient pulses, and immediately before phase encoding. In the case of purely linear motion along the direction of the motion-sensitizing gradients (e), the signal amplitude is unchanged, but the signal phase changes. With other forms of motion (f), both signal amplitude and phase changes occur.

to compensate (*18*). By restriction of the volume of interest to regions with simple motion patterns (preferably linear motion), phase cancellation effects due to nonuniform motion are reduced. In brain, such nonuniform movements may be due to cardiac-related pulsations (*12–14*). Cardiac gating to periods of minimum movements helps to reduce artifacts from these movements (*15*).

Measurements were performed on a clinical 1.5 T Signa scanner (General Electric Co., Milwaukee, Wisconsin) equipped with actively shielded gradients of 10 mT/m maximum strength. A standard quadrature head coil was used.

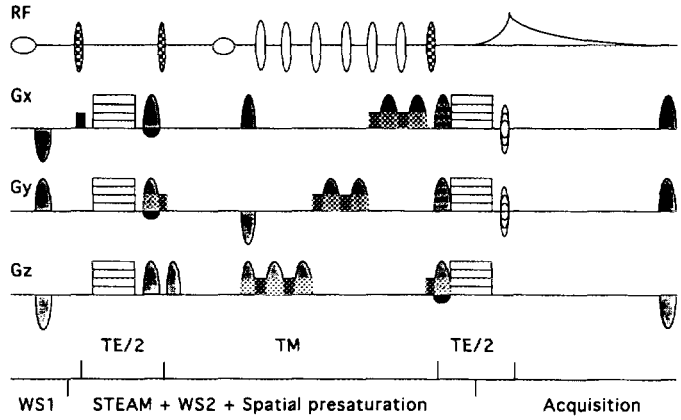

FIG. 2. Localized proton spectroscopic-imaging pulse sequence based on STEAM inner-volume selection and outer-volume suppression during TM. CHESS water suppression pulses are applied before the STEAM localization (WS1) and during TM (WS2) prior to spatial suppression. Suppression RF pulses are depicted as open symbols. The STEAM RF pulses are shown in black and white checks. Slice-selection gradients and rephasing gradients are in black, and gradient-dephasing pulses are in gray. Additional motion-sensitizing gradients with variable amplitudes are applied during the TE/2 intervals. Phase-encoding gradients are applied immediately before the center of the echo. Data acquisition starts before the application of phase-encoding gradients.

Spectroscopic volume prelocalization of an 8 × 8 × 2 cc volume was obtained with a water-suppressed stimulated-echo pulse sequence (Fig. 2) (*6, 9–11, 15*). Measurements were performed with TR = 4 s, TE = 65 ms, and TM = 200 ms. Optimized volume localization was obtained by combining STEAM inner-volume excitation with complete outer-volume suppression as described previously (*6, 15*). Outer-

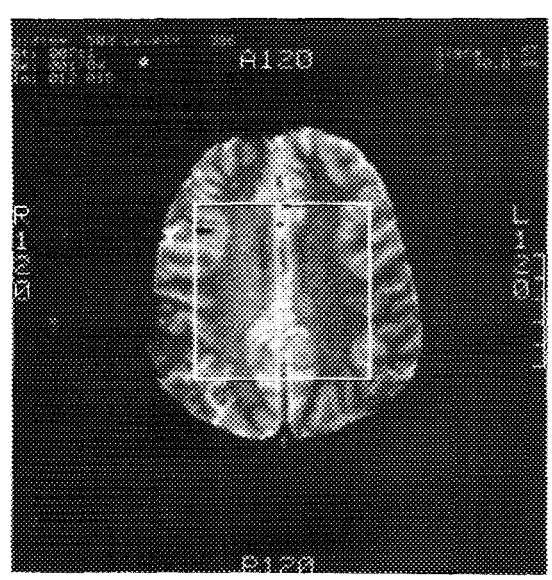

FIG. 3. Axial GRASS localizer indicating the spectroscopic volume prelocalization in human brain (TR = 600 ms, TE = 5 ms, flip angle = 45°).

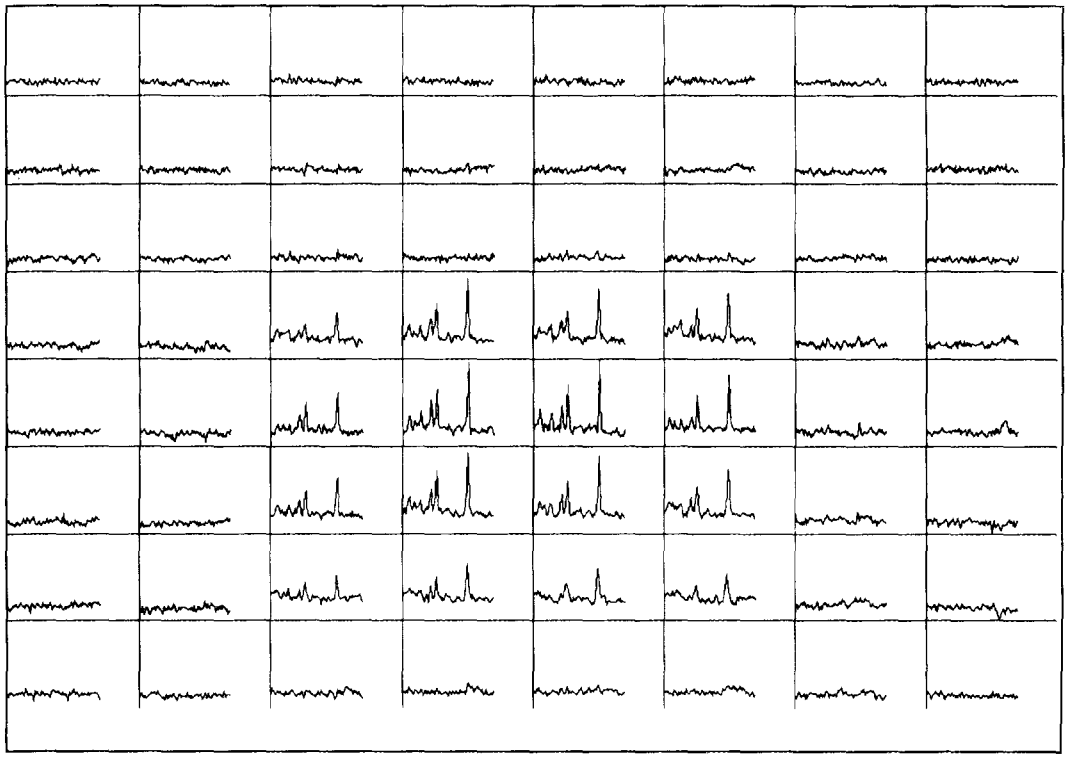

FIG. 4. Spectroscopic imaging data acquired *in vivo* without additional motion-sensitizing gradients. Motion artifacts are negligible when conventional data reconstruction is used. Absorption-mode spectra display the spectral range from 0 to 4 ppm. Three major resonances from choline-containing compounds, creatine/phosphocreatine, and *n*-acetyl aspartate (from left to right), as well as several less intense resonances from compounds such as inositols, are visible in individual spectra (TR = 4 s, TE = 65 ms, TM = 200 ms, FOV = 20 cm, 8 × 8 matrix, slice thickness = 2 cm, one excitation per phase-encoding step, peripheral gating).

volume suppression was applied during the TM period to minimize the time delay between the spatial suppression and the signal acquisition. For *in vivo* experiments, water suppression was obtained by two chemical-shift-selective pulses [CHESS (*25*)]. The dephasing gradient pulses for volume prelocalization during the TE/2 intervals had a duration of 4 ms. Additional motion-sensitizing gradients of 18 ms width were purposely applied along the x, y, and z axes (simultaneously) during the TE/2 intervals. Two-dimensional spectroscopic images with a matrix size of 8 × 8 voxels covering a field of view of 20 cm were acquired in axial orientations. Phase-encoding gradients of 1 ms width were applied immediately before the top of the echo. No signal averaging was used. Signal acquisition using a spectral width of 1 kHz and a digital resolution of 1 Hz started immediately after the motion-sensitizing gradient pulses. For comparison, spectral reconstruction was performed without motion compensation, with compensation of phase errors only, and with compensation of both phase and amplitude error as described above using the SAGE spectral analysis software (General Electric Co.).

In vivo measurements on eight normal volunteers (five male, three female) ranging in age from 22 to 32 years were obtained after informed consent. Measurements were repeated on two volunteers. Preselected volumes were either located above the ventricles mostly containing white matter (Fig. 3) or at the level of the lateral ventricles. Peripheral gating with a time delay of 300 ms between the systolic wave and the pulse sequence trigger was found to minimize cardiac-related signal amplitude variations (*15*). Water suppression was adjusted to leave a residual water signal which dominated the spectrum and served as a tracer signal for signal postprocessing. A specially designed head holder limited involuntary head movements. Thus, view-to-view motion artifacts were minimal. Data sets obtained without motion-sensitizing gradients could be reconstructed with conventional methods. Typical localized spectra displaying the spectral range from 0 to 4 ppm with resonances from *n*-acetylaspartate (2.01, 2.52 ppm), glutamine/glutamate (2.35, 3.8 ppm), creatine/phosphocreatine (3.02, 3.93 ppm), choline-containing compounds (3.24 ppm), and inositols (3.54 ppm) are shown in Fig. 4 (*26*). With increasing motion-sensitizing gradient strength, the degree of motion artifacts in conventionally reconstructed data sets increased strongly. In all subjects studied, metabolite localization was almost completely lost when maximum gradient strengths were ap-

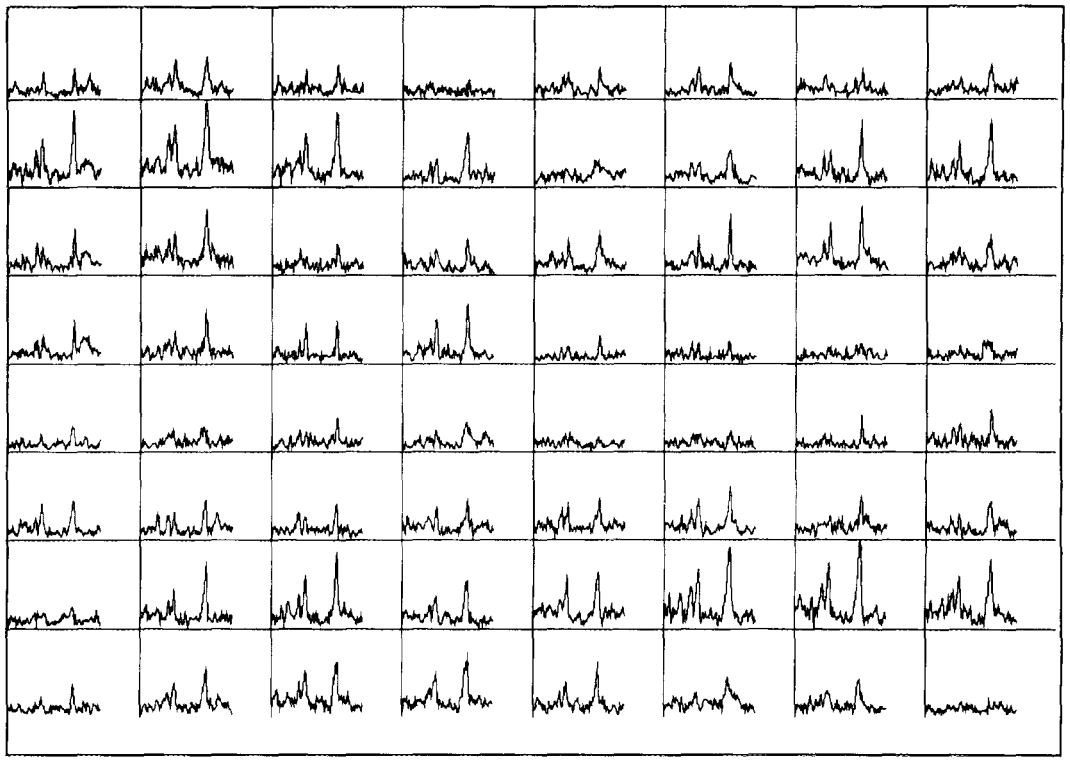

FIG. 5. Data set acquired under the same conditions as those given in the legend to Fig. 4 except for the application of additional motion-sensitizing gradients of 18 ms width and 10 mT/m strength. Conventional MRSI data reconstruction results in strong motion artifacts.

plied (Fig. 5). Under the chosen experimental conditions, even small displacements with velocities on the order of 1 mm/s would lead to significant phase-encoding errors. It is likely that both cortical brain pulsations which are predominantly cephalocaudal (superior–inferior) in direction (*12–14*) and involuntary movements of the whole head contributed to these artifacts. Since our acquisitions were triggered to periods of minimum brain pulsations where cortical velocities are less than 0.3 mm/s (*13*), involuntary head movements were probably the major source of artifacts. With both zero-order phase correction and combined signal phase and amplitude normalization, motion artifacts were strongly reduced (Fig. 6).

The spectral quality of motion-compensated data sets was comparable to that of conventionally reconstructed data sets acquired without motion sensitization. Phase-error compensation removed the majority of motion artifacts indicating major contribution from linear movements. As expected, combined phase and amplitude error correction usually gave slightly better localization. However, in some cases, the amplification of noise in individual raw data traces which suffered from strong signal losses due to nonlinear or nonuniform motion introduced additional artifacts in the spectroscopic images. To reduce such noise artifacts, it may be necessary to limit the gain increase in individual raw data traces. Spectroscopic images acquired at different slice locations in brain tissue indicated that our motion-compensation method is most robust in areas with homogenous motion patterns such as in the posterior fossa.

While the examples presented here demonstrate extreme cases of motion sensitivity, motion artifacts with clinical MRSI are usually less pronounced. However, small localization errors from intense signals such as from residual water or from superficial lipids may still introduce substantial spectral artifacts and impair quantitation of individual resonances. For example, our experience with measurements on infants (*27*) indicates that sudden head movements may introduce significant phase errors in individual acquisitions. Generalized reconstruction techniques with optimized point-spread functions, such as Fourier series windows (*28*) or SLIM (*29*), which are particularly sensitive to motion-induced phase errors, may benefit from motion compensation as well. Our signal-tracking method may also be useful to reduce motion artifacts in diffusion-sensitive MRSI. We are currently investigating the possibility of mapping the diffusion coefficients of individual metabolite resonances by MRSI. Similar measurements using single-voxel methods have recently been performed in animal (*30, 31*) and human brain (*15*). In addition to motion-related localization arti-

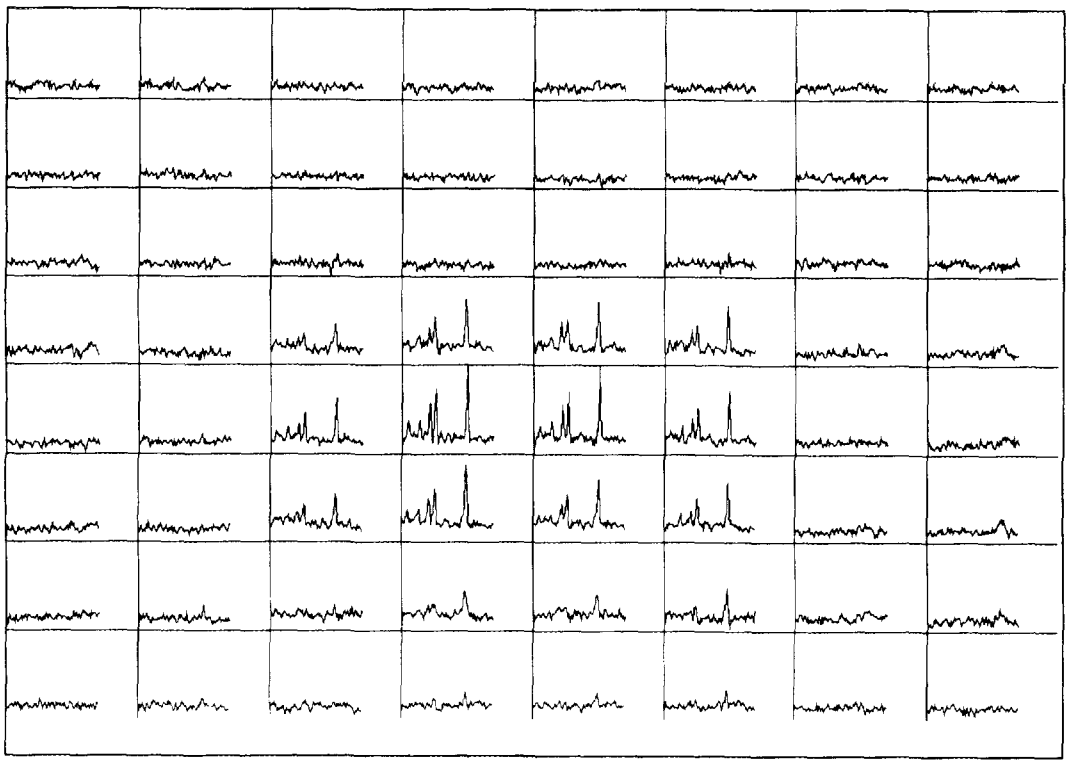

FIG. 6. Same data set as that in Fig. 5 reconstructed with motion compensation using both phase and amplitude error compensation in individual raw data traces. Spectroscopic localization is completely recovered and similar to that obtained without additional motion-sensitizing gradients (Fig. 4).

facts, our method will also compensate signal errors due to RF instabilities.

For conventional imaging, similar motion-compensation methods which detect signal errors in a so-called navigator echo prior to the imaging echo have been proposed (*18–23*). The object projection generated from the navigator echo allows for correction of view-to-view displacements while phase errors in the navigator echo are extrapolated to estimate phase errors in the imaging echo. Such methods are prone to extrapolation errors in case of nonuniform movements. With our method the possibility of extrapolation errors is significantly reduced, since signal errors are detected immediately before the center of the echo.

ACKNOWLEDGMENTS

The authors gratefully thank Dr. Joseph A. Frank (LDRR, NIH) for supporting this work. The Swiss National Science Foundation has supported one of the authors (S.P.) through a research stipend.

REFERENCES

1. P. R. Luyten, A. J. H. Marien, W. Heindel, *et al., Radiology* **176,** 791 (1990).
2. D. L. Arnold, P. M. Matthews, G. S. Francis, J. O'Connor, and J. P. Antel, *Ann. Neurol.* **31,** 235 (1992).
3. K. Herholtz, W. Heindel, P. R. Luytens, *et al., Ann. Neurol.* **31,** 319 (1992).
4. H. Kugel, W. Heindel, R. I. Ernestus, J. Bunke, R. du Mesnil, and G. Friedman, *Radiology* **183,** 701 (1992).
5. J. H. Duijn, G. B. Matson, A. A. Maudsley, J. W. Hugg, and M. W. Weiner, *Radiology* **183,** 711 (1992).
6. S. Posse, B. Schuknecht, M. E. Smith, P. C. M. van Zijl, N. Herschkowitz, and C. T. W. Moonen, *J. Comput. Assist. Tomogr.* **17,** 1 (1993).
7. P. A. Bottomley, U.S. Patent 4 480 228, 1984.
8. R. J. Ordidge, M. R. Bendall, R. E. Gordon, and A. Connelly, in "Magnetic Resonance in Biology and Medicine" (Govil, Khetrapal, and Saran, Eds.), p. 387, Tata McGraw–Hill, New Delhi, India, 1985.
9. J. Granot, *J. Magn. Reson.* **70,** 488 (1986).
10. R. Kimmich and D. Hoepfel, *J. Magn. Reson.* **72,** 379 (1987).
11. J. Frahm, K. D. Merboldt, and W. Hänicke, *J. Magn. Reson.* **72,** 502 (1987).
12. D. A. Feinberg and A. S. Mark, *Radiology* **163,** 793 (1987).
13. B. P. Poncelet, V. J. Weeden, R. M. Weisskopf, and M. S. Cohen, *Radiology* **185,** 645 (1992).
14. D. R. Enzmann and N. J. Pelc, *Radiology* **185,** 653 (1992).
15. S. Posse, C. A. Cuenod, and D. Le Bihan, *Radiology,* in press.
16. E. M. Haacke and J. L. Patrick, *Magn. Reson. Imaging* **4,** 359 (1986).
17. G. W. Lenz, E. M. Haacke, and R. D. White, *Magn. Reson. Imaging* **7,** 445 (1989).
18. R. L. Ehman and J. P. Felmlee, *Radiology* **173,** 255 (1989).

19. J. P. Felmlee, R. L. Ehman, S. J. Riederer, and H. W. Korin, *Magn. Reson. Med.* **18,** 207 (1991).
20. J. P. Felmlee, R. L. Ehman, S. J. Riederer, and H. W. Korin, *Radiology* **179,** 139 (1991).
21. R. J. Ordidge, J. A. Helpern, Z. Qing, and R. A. Knight, Abstracts of the Society of Magnetic Resonance in Medicine, 11th Annual Meeting, p. 1209, 1992.
22. J. Wilbrink, L. H. Zang, J. Fielden, A. Takane, and H. Koizumi, Abstracts of the Society of Magnetic Resonance in Medicine, 11th Annual Meeting, Works in Progress, p. 481, 1992.
23. R. Asato, T. Tsukamoto, R. Okumura, Y. Miki, E. Yoshitome, and J. Konishi, Abstracts of the Society of Magnetic Resonance in Medicine, 11th Annual Meeting, Works in Progress, p. 1226, 1992.
24. I. R. Young, I. D. Cox, G. A. Coutts, and G. M. Bydder, *NMR Biomed.* **2,** 329 (1989).
25. A. Haase, J. Frahm, W. Haenicke, and D. Matthaei, *Phys. Med. Biol.* **30,** 341 (1985).
26. C. Arus, Y. Chang, and M. Barany, *Physiol. Chem. Phys. Med. NMR* **17,** 23 (1985).
27. P. S. Hüppi, S. Posse, F. Lazeyras, R. Burri, E. Bossi, and N. Herschkowitz, *Ped. Res.* **30,** 574 (1991).
28. T. H. Mareci and H. R. Brooker, *J. Magn. Reson.* **57,** 157 (1984).
29. X. Hu, D. N. Levin, P. C. Lauterbur, and T. Spraggins, *Magn. Reson. Med.* **8,** 314 (1988).
30. C. T. W. Moonen, P. van Gelderen, P. C. M. van Zijl, D. DesPres, and A. Olson, Abstracts of the Society of Magnetic Resonance in Medicine, 10th Annual Meeting, p. 141, 1991.
31. K. D. Merboldt, D. Höstermann, H. Bruhn, W. Hänicke, and J. Frahm, *Magn. Reson. Med.* **29,** 125 (1993).